High Throughput Synthesis and Screening of New Catalytic Materials for the Direct Epoxidation of Propylene

Michael Kahn[1], Anusorn Seubsai[1], Isik Onal[2] and Selim Senkan[*,1]

[1]*Department of Chemical Engineering, University of California, Los Angeles, CA 90095, USA*

[2]*Department of Chemical Engineering, METU Ankara, Turkey*

Abstract: Nanoparticles of 35 individual metals as well as their binary combinations were synthesized using High Throughput pulsed laser ablation (PLA), and collected on Al_2O_3, CeO_2, SiO_2, TiO_2, and ZrO_2 pellets. These materials were then screened for their catalytic activities and selectivities for the partial oxidation of propylene, in particular for propylene oxide (PO), using array channel microreactors. Reaction conditions were the following: 1 atm pressure, gas hourly space velocity (GHSV) of 20,000 h^{-1}, temperature 300°C, 333°C, and 367°C, and feed gas composition 20 vol% O_2, 20 vol% C_3H_6 and balance He. Initial screening experiments resulted in the discovery of SiO_2 supported Cr, Mn, Cu, Ru, Pd, Ag, Sn, and Ir as the most promising leads for PO synthesis. Subsequent experiments pointed to bimetallic Cu-on-Mn/SiO_2, for which the PO yields increased several fold over single metal catalysts. For multimetallic materials, the sequence of deposition of the active metals was shown to have a significant effect on the resulting catalytic activity and selectivity.

Keywords: Heterogeneous catalysis, partial oxidation, laser ablation, nanoparticles, array micro-reactors.

1. INTRODUCTION

Propylene oxide (PO) is an important intermediate used in the synthesis of a large variety of valuable consumer products such as urethane forms, polymers, cosmetics, and food emulsifiers and additives. Over 10 billion pounds of PO are produced annually, using two major technologies—the chlorohydrin and hydroperoxide processes [1]. However, both of these processes are laden with serious economic, health and ecologic drawbacks. The chlorohydrin process requires the use of chlorine, which is a toxic and corrosive reagent, and can produce additional toxic chlorinated organic by-products. The hydroperoxide process produces co-products, such as the styrene monomer, thereby linking the economic viability of PO production to the market value of the co-product. Recently, a new PO synthesis route based on the in-plant production of H_2O_2 is also being commercialized [2]. Nevertheless, the direct synthesis of PO from propylene and molecular oxygen remains one of the most challenging goals of industrial catalysis.

To date, a large variety of heterogeneous and homogeneous catalysts, and in particular supported metal catalysts have been investigated for the title reaction using different techniques [3-16, also 2 and references therein]. Notably, silver and palladium were explored [3-6], but the most attention has been given to gold nanoparticles, e.g., Au/TiO_2 and Au/TS-1 [2, 4, 7-13]. The latter was shown to exhibit high selectivity (50-90%) towards PO production. However, gold catalysts utilize hydrogen as a co-reactant for PO synthesis, rendering this process less desirable for industrial implementation. Most recently, copper was reported to be effective in the direct production of PO, without hydrogen, although the initial yields were below those required for commercial interest [14].

The lack of a breakthrough in propylene epoxidation catalysis, in spite of world-wide efforts, clearly suggests the need to develop novel approaches for catalyst research and development. This fact, coupled with the abundance of catalytic materials that must be explored to discover new leads, e.g., binary, ternary and higher order combinations of metals as well as a large variety of support materials, call for the application of combinatorial or high throughput heterogeneous catalysis tools and methods. Our laboratories made pioneering contributions to this field through the development of novel High Throughput catalyst preparation and screening tools [17-21]. In particular, we developed array channel micro-reactors to rapidly screen a large numbers of catalytic materials in parallel [17, 18]. In addition, we coupled these array reactors to laser spectroscopy [17], photoionization detection (PID) [17], mass spectrometry [19], and fast gas chromatography [20]. Recently, we also developed a High Throughput pulsed laser ablation (HT-PLA) system for the synthesis of uniformly sized single- and multi-metallic nanoparticles for catalytic applications [21]. Research in combinatorial and High Throughput catalysis technologies continues to expand globally, as evidenced by the latest *EuroCombiCat* meeting which took place in Bari, Italy in 2007, in which remarkable discoveries and optimization of new catalysts for a wide variety of applications were reported [22]. It is interesting to note that the US academic community, in particular chemical engineering where the majority of heterogeneous catalysis research is performed, is not engaged in the development and/or use of combinatorial and High Throughput technologies. Advances in high throughput catalysis were also the subject of several review articles published recently [23, 24].

*Address correspondence to this author at the Department of Chemical Engineering, University of California, Los Angeles, CA 90095, USA;
E-mail: senkan@ucla.edu

1386-2073/10 $55.00+.00

Here we report on the results of a comprehensive and systematic investigation of the catalytic properties of supported nanoparticles of 35 individual metals prepared by HT-PLA for the direct synthesis of PO from propylene and oxygen. Initial screening experiments resulted in both confirmatory findings (e.g., Cu, Ag, and Pd) and new discoveries of SiO_2 supported Cr, Mn, Ru, Sn, and Ir. Subsequent studies of the bimetallic Mn and Cu system, also supported on SiO_2 has led to a remarkable improvement of the PO yield, by nearly a factor of 5 when compared to single-component catalysts. These findings not only suggest the use of multi-metallic systems for direct propylene epoxidation catalysis, but also provide a clear demonstration of the utility of High Throughput techniques for catalyst discovery and optimization.

2. EXPERIMENTAL

Catalytic materials were prepared by depositing nanoparticles of metals on Al_2O_3, CeO_2, SiO_2, TiO_2, and ZrO_2 supports using the High Throughput pulsed laser ablation (HT-PLA) system shown in Fig. (**1**), the details of which have been described recently [21]. Briefly, the HT-PLA system consists of 24 rotatable and interchangeable metal targets and 30 interchangeable substrates housed in a vacuum chamber with optical access to a laser beam. The laser beam (Lambda Physik Compex 100 KrF Excimer Laser, 300mJ/pulse, 30 ns pulse duration) is then focused to a spot of ~0.1 cm diameter, off axis on the surface of the target, arriving at an angle of approximately 45°. Nanoparticles emanating from the target were collected on one of the flat surfaces of the support pellets (0.4 cm diameter by 0.1 cm thick cylinders) by placing the pellets inside the ablation plume at a pre-determined distance from the target. The HT-PLA vacuum chamber was maintained at 1.0 torr Ar pressure, and a grounded mask was used to prevent cross contamination of different support pellets. All PLA targets were pre-cleaned *in situ* by ablating the topmost layer of material onto an unused substrate. As demonstrated earlier [21], PLA allows the synthesis of uniformly sized nanoparticles with diameters decreasing with increasing distance from the target, with remarkably narrow particle size distribution. These features are illustrated by the transmission electron microscope (TEM) images of Rh nanoparticles shown in Fig. (**2**). It should be noted that the nanoparticles are deposited on the external surfaces of the pellets, with little penetration into the pores. Nanoparticles created initially will be in zero-valent metal form as they are generated in an argon atmosphere. However, upon exposure to air and/or reaction conditions, certain metals would become oxidized.

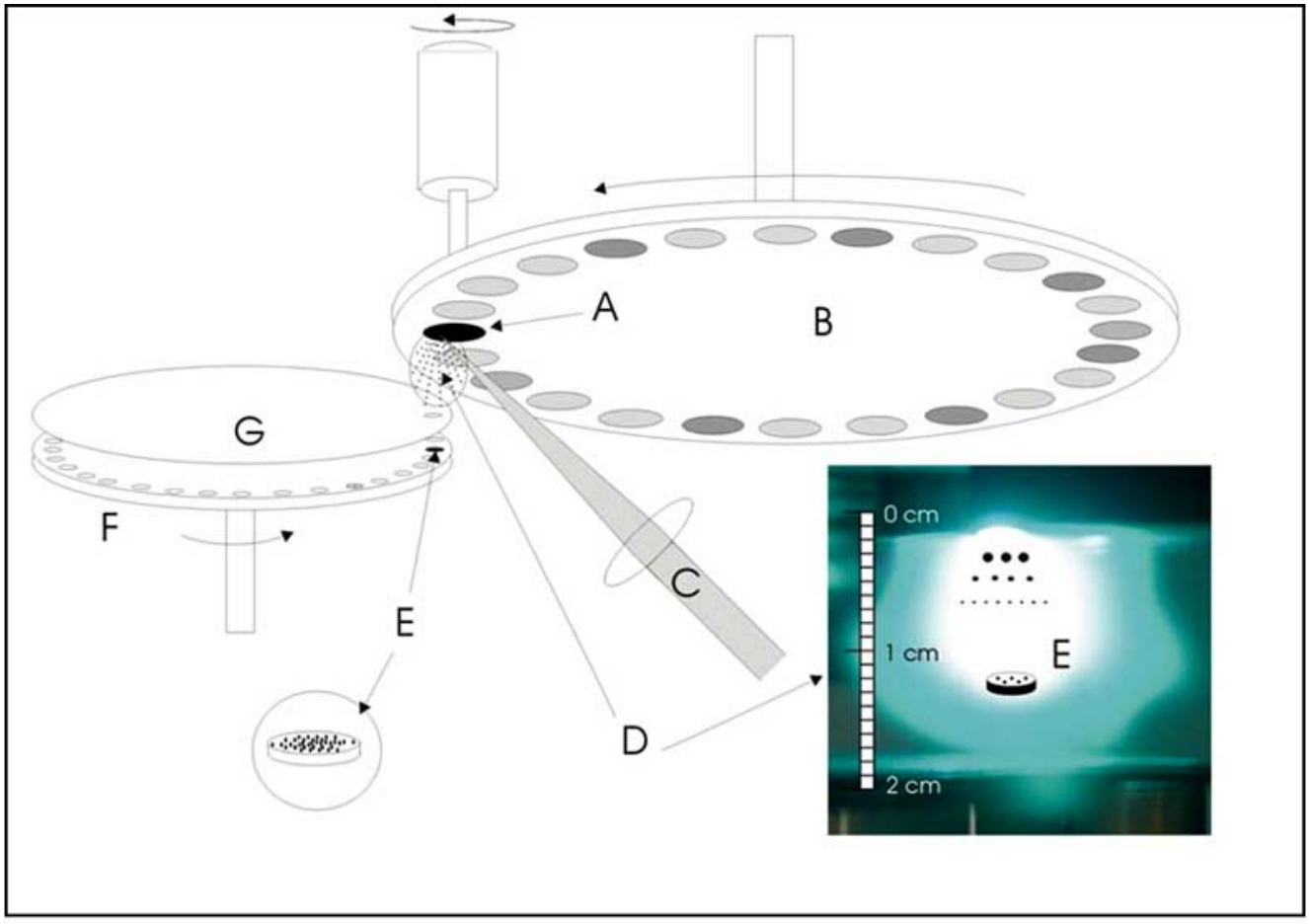

Fig. (1). High Throughput Pulsed Laser Ablation (HT-PLA) system. **A**. Metal target; **B**. Rotating target holder; **C**. Pulsed laser beam; **D**. Ablation plume; **E**. Nanoparticle collection surface (e.g., catalyst support pellet or TEM grid with film; **F**. Rotating support pellet holder; **G**. Mask.

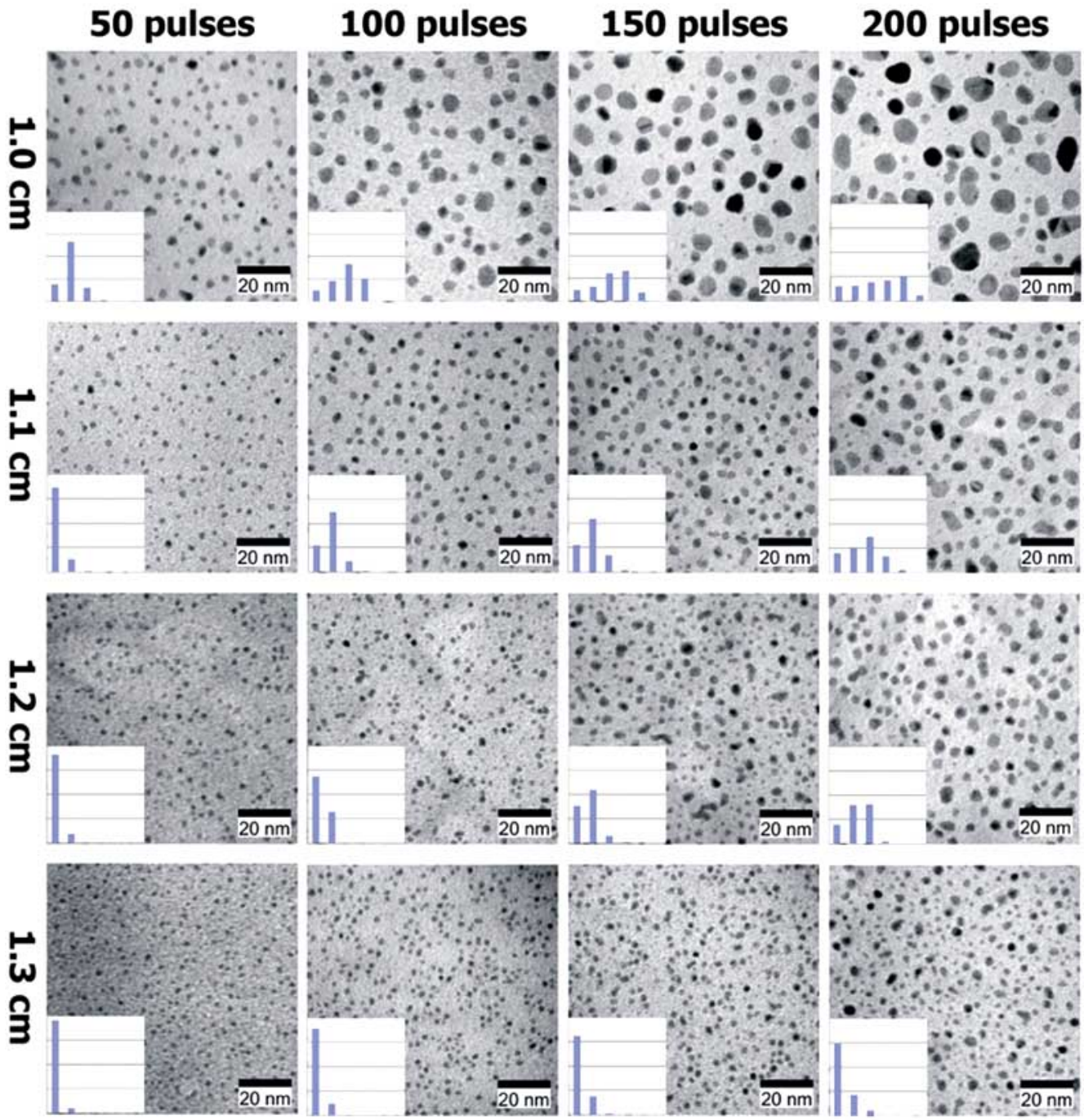

Fig. (2). TEM images of rhodium nanoparticles prepared by pulsed laser ablation. As evident from this figure, diameters of nanoparticles collected on substrates uniformly decreased with increasing distance from target at a fixed number of laser pulses (from top to bottom), and increased with increasing pulse numbers at a fixed distance from the target (from left to right) [21]. The histogram inserts illustrate a narrow particle size distribution.

In the first, i.e. discovery phase, a library of 35 distinct unimetallic catalytic materials was prepared by ablating pure metal targets (min 99.99% purity) that were either foils or thin disks prepared by pressing and high-temperature sintering (500^{o}C under Ar) powders of pure metals. For each metal, 2 sets of catalytic materials were prepared by depositing 100 laser pulses of nanoparticles onto support pellets at 2 different target-to-substrate distances. This was undertaken in order to explore the effects of nanoparticle size on selectivity and conversion, at the same metal loading, since the diameters of nanoparticles collected on substrates significantly decrease with increasing distance from the target [20, 21]. Other laser properties were maintained constant. It should be noted that metal loading increases with increasing number of laser pulses for the same metal. However, since ablation rates of the targets are metal specific, due to differences in melting and boiling points, density, surface reflectivity etc., nanoparticle loadings of the support materials will be different for different metals.

In the second phase, bimetallic catalytic materials were prepared using the leads discovered from the reaction

screening of the initial library of unimetallic catalytic materials. Promising bimetallic systems subsequently were investigated in greater detail in an attempt to develop superior bimetallic catalysts as well as to optimize operating conditions for the title reaction.

Catalyst evaluations were performed using our computer controlled array channel microreactor system shown in Fig. (**3**), details of which were reported previously [17]. In this system, up to 80 catalysts can be screened in parallel. In the array microreactors used, reactant gases flow over the flat surfaces of nanoparticle-coated support pellets which are individually placed inside cylindrical wells and are isolated within reactor channels; the flow regime was similar to that of a monolithic reactor [20]. All experiments were performed under atmospheric pressure and at a gas hourly space velocity (GHSV) of 20,000 h^{-1}, representing differential reactor conditions. GHSV was calculated using the gas flow rate and the volume of the catalyst pellet used in each channel. Support pellets without metal loading were placed in empty channels to ensure uniform gas distribution within the array. Initial screening experiments were performed at temperatures of 300°C, 333°C, and 367°C using a feed gas composition of 20 vol% O_2, 20 vol% C_3H_6 and balance He. Reactor effluent gases were analyzed by withdrawing the products using a heated capillary sampling probe followed by on-line gas chromatography (Varian CP-4900 Micro GC with thermal conductivity detector, Porapak Q (10m) and Molecular sieve 13X (10m) columns). Sensitivity of the GC was about 20 parts per million (ppm), well below the levels of all products formed in the reaction process. Reproducibility of the measurements were explored and they were within $\pm$10%. GC calibrations were made using standard gas mixtures prepared separately from pure compounds. Concentrations of the species in the calibration mixtures were kept as close to reactor exit conditions to ensure accurate quantification.

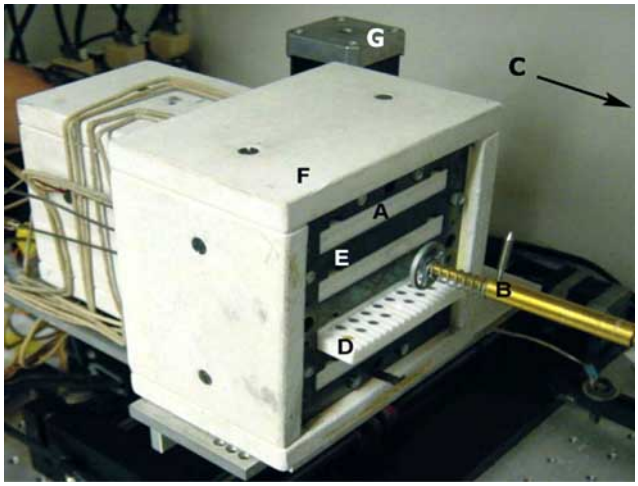

Fig. (3). Array channel micro-reactor system used in the High Throughput screening of new catalytic materials. **A**. Reactor array with 20 channels; **B**. Heated gas sampling probe; **C**. Gas chromatograph and/or mass spectrometer; **D**. Catalytic materials placed inside the wells of the reactor array; **E**. Stainless steel heating block; **F**. Insulation; **G**. Stepper motor for the micro-positioning of the reactor block.

3. RESULTS AND DISCUSSION

Early scoping experiments with PO in the feed revealed that among the 5 support materials considered (i.e. Al_2O_3, CeO_2, SiO_2, TiO_2, and ZrO_2), SiO_2 held the most promise in preserving the PO produced under the reaction conditions. This result is in harmony with the literature on propylene epoxidation catalysis [15]. Consequently, we focused our research on metal nanoparticles supported on SiO_2. In Fig. (**4**), selected results for the unimetallic nanoparticle catalyst screening experiments, completed in a time frame of about 2 weeks, are presented in a periodic table format for all of the 35 metals considered. For each element, reactor exit PO mole fractions (y-axis) are plotted as a function of temperature (x-axis). The results in the background correspond to nanoparticles collected at distances closer to the target, i.e. larger particles (see Fig. **2**). In the cases of Pd and Ag, nanoparticles were collected at 3 different locations in the ablation plume.

An inspection of Fig. (**4**) clearly indicates SiO_2 supported Cr, Mn, Cu, Ru, Pd, Ag, Sn, and Ir are the most promising leads for PO synthesis among the 35 metals considered. Cu, Pd and Ag were previously reported to be active towards PO synthesis [3-6,14]; thus it is gratifying that our high throughput methods were able to confirm these earlier findings. On the other hand, Cr, Mn, Ru, Sn and Ir represent new leads of catalytic materials for the direct synthesis of PO from propylene and oxygen.

As noted earlier, the purpose of these screening experiments was to rapidly identify *new leads* for catalytic materials that promote the direct synthesis of PO *via* propylene and molecular oxygen. Consequently, the operating conditions for all the catalysts investigated have not been optimized; but this is a relatively straight forward process once new leads are discovered. In addition, none of the results presented in Fig. (**4**) are likely to have an immediate industrial impact due to low conversions attained, i.e. differential reactor operating conditions were used. For example, while Pd produced PO at the highest levels among all the catalysts investigated, PO selectivity (defined as the percent of carbon in PO among all the products) was still below 2% because of excessive CO_2 formation, rendering Pd unsuitable as a PO catalyst. Therefore the challenge clearly remains to increase PO production rates while also increasing PO selectivity. We addressed this need in the second phase of the program by focusing on the leads Mn and Cu, together with their binary combinations Mn+Cu, because these metals exhibited the highest selectivity for PO production. Other lead metals are currently under investigation and will be reported in the future.

Unimetallic Mn and Cu catalysts with different metal loadings were prepared by depositing nanoparticles of individual metals on the SiO_2 support for laser pulses from 10 to 500, while maintaining the target-to-substrate distance at 0.8 cm and other operating conditions the same as stated earlier. Based on TEM characterization of Mn and Cu nanoparticles created by PLA, the weight of catalyst collected on a 0.4 cm disc is estimated to be 30ng Cu/pulse and 12ng Mn/pulse at these conditions. Mn+Cu bimetallic catalysts were prepared by the *sequential deposition* process. In this case, the first set of metal nanoparticles, i.e. the under-layer, was deposited directly over the SiO_2 support at

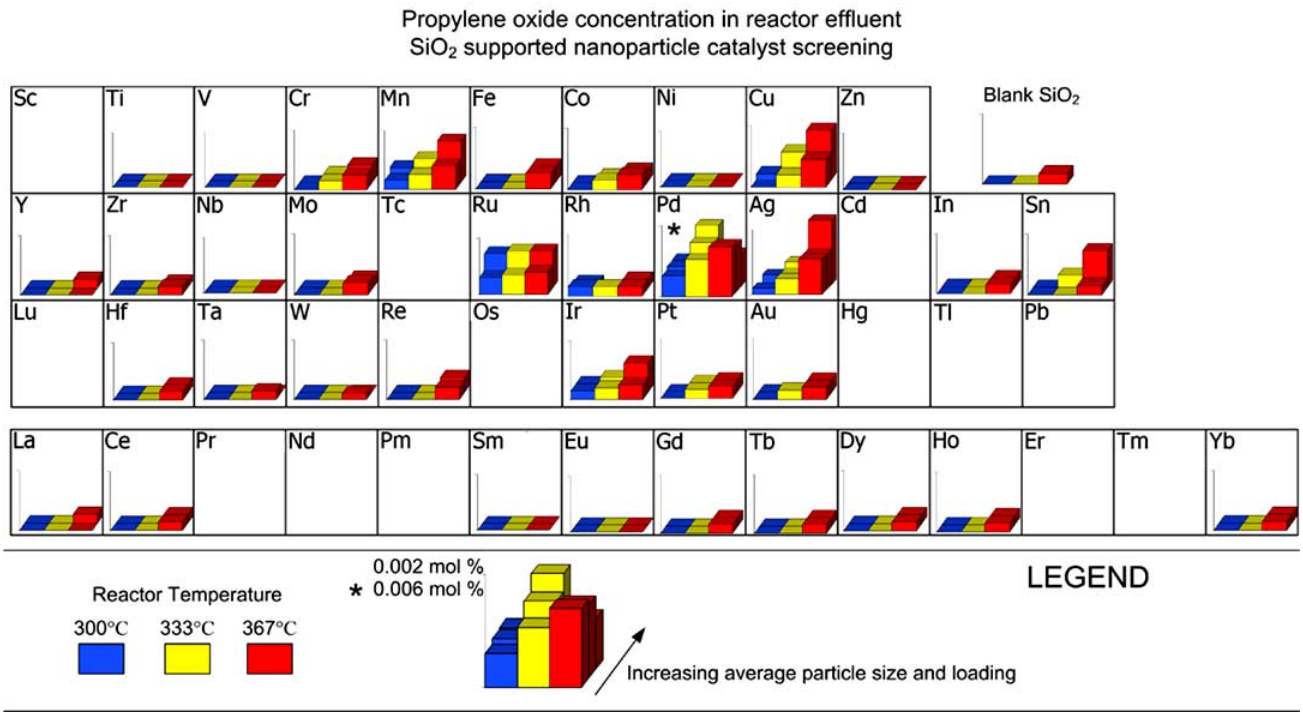

Fig. (4). Unimetallic SiO_2-supported nanoparticle catalyst screening results. The purpose of these experiments was to identify catalyst leads for the direct synthesis of propylene oxide by rapidly screening large number of catalytic mateirals. Detailed analysis was not pursued for these catalysts due to the more pressing issue of finding suitable bimetallic catalysts.

a fixed loading level corresponding to 500 laser pulses. This was followed by the deposition of the second metal layer (i.e. the top-layer), the loading of which was systematically varied from 10 to 500 laser pulses.

In Fig. (**5**), PO selectivities are presented as a function of propylene conversions for the unimetallic and bimetallic Mn and Cu catalysts explored in phase 2 at a temperature of 375°C, GHSV of 20000 h^{-1}, and a feed gas composition of 26% C_3H_6, 14% O_2, and balance He. These conditions were found to be more favorable than the conditions used in the initial screening experiments. An inspection of Fig. (**5**) reveals several important results. First, both unimetallic Mn/SiO_2 (■) and Cu/SiO_2 (♦) catalysts exhibited inferior PO yields (PO yield = PO selectivity x Propylene conversion), regardless of the metal loading, when compared to bimetallic results discussed below. For example, the Mn/SiO_2 (■) data points for 10 to 500 laser pulses were all grouped together at the lower left side of the graph, i.e. closest to the origin. As seen from Fig. (**5**), PO selectivity increased slightly with Mn loading reaching a maximum of about 8% at 500 pulses (6 μg Mn). The results for Cu/SiO_2 (♦) were slightly better, with PO selectivities reaching 17% at 300 pulses (9 μg Cu). However, in both cases propylene conversions were in the range of 0.2-0.4%.

The most remarkable result shown in Fig. (**5**) is the fact that for the bimetallic Cu-on-Mn/SiO_2 (▲) catalysts *PO yields were higher by a factor of 5* than the corresponding unimetallic catalysts. These improved bimetallics exhibit PO selectivities as high as 22% at propylene conversions of 1%. This is a surprising result, since the combination of copper and manganese oxides has been used in the past as a total oxidation catalyst [25, 26]. It is also significant to note that Cu-on-Mn/SiO_2 (▲) was also superior to the bimetallic Mn-on-Cu/SiO_2 (○) catalysts for the synthesis of PO. This result clearly demonstrates the importance of the order of deposition of the metals in bimetallic catalysts in order to affect the desired catalysis action.

Finally in Fig. (**6**), the complete product yields are presented for the catalysts Cu-on-Mn/SiO_2 (Fig. **6A**), Mn-on-Cu/SiO_2 (Fig. **6B**), together with the same for unimetallic catalytic materials Cu/SiO_2 (Fig. **6C**) and Mn/SiO_2 (Fig. **6D**) at 375°C. As evident from Fig. (**6A**), product yields exhibit a clear optimum with regard to Cu loading for the Cu-on-Mn/SiO_2 catalysts, with maximum PO yield observed at 70 pulses, corresponding to 2 μg Cu on 6 μg Mn. A closer inspection of Fig. (**6A**) also shows that acrolein (AC) was the other major C_3 product with a selectivity of about 22%, followed by acetone (AT) at 4%. Note that the AC signal typically includes a trace amount of propionaldehyde (PaL) due to PO isomerization. However, CO_2 was the most abundant product formed in Cu-on-Mn/SiO_2 catalysis reaching selectivities in excess of 50%. These results eagerly demonstrate the need to further improve the performance of this catalytic material.

In contrast, the product mix for Mn-on-Cu/SiO_2 catalysts (Fig. **6B**) was dominated by AC and this was entirely due to Cu being the under-layer. In fact, AC selectivities dramatically decreased from 60% on the Cu/SiO_2 surface (zero Mn pulses) to a value of 17 % when 300 pulses on Mn were deposited. Increased coverage of the Cu sites by Mn can readily account for these results. These findings are also consistent with those observed on unimetallic Cu/SiO_2 catalysts (Fig. **6C**), where AC selectivities steadily increased to 60% upon increasing the Cu loading to 500 pulses. It is interesting to note, however, that PO yields were not strongly influenced by the Mn loading on the Mn-on-

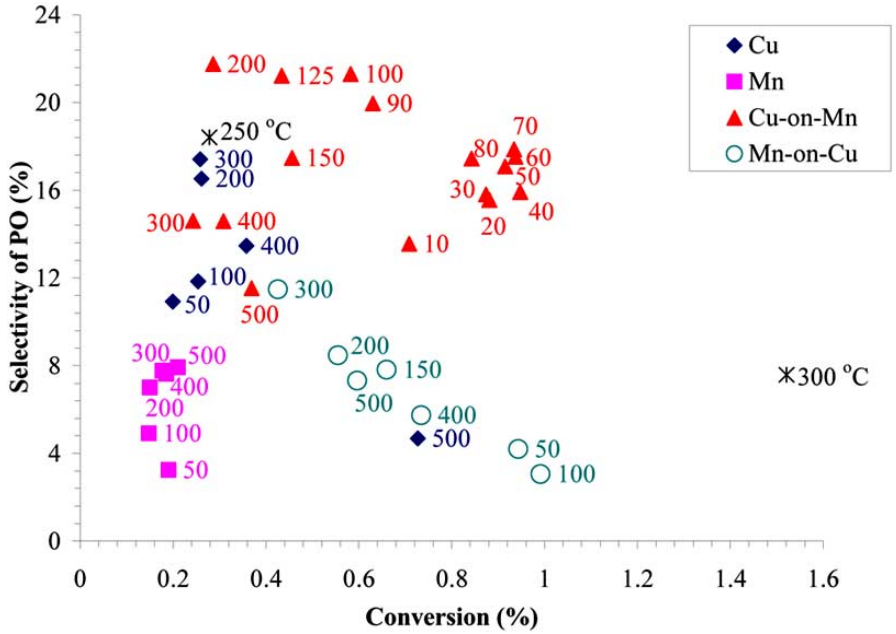

Fig. (5). Selectivity versus conversion chart at 375 °C. The numbers next to the data points represent the variable number of pulses of the topmost catalyst layer (see text). Considerable improvement of bimetallic Cu-on-Mn (▲) catalysts is apparent when compared with unimetallic Mn (■) and Cu (♦) catalysts. Note that Cu-on-Mn (▲) is superior to Mn-on-Cu (○). Points indicated by temperatures (∗) correspond to 5% Cu/SiO_2 catalysts prepared by impregnation [14].

Cu/SiO_2 catalysts (Fig. **6B**); PO selectivities remained at about 8% above 150 pulses of Mn. Carbon dioxide still remained a significant product formed by this catalyst. Unimetallic Mn/SiO_2 catalysts were essentially total oxidation catalysts, with the production of only low levels of AC (Fig. **6D**).

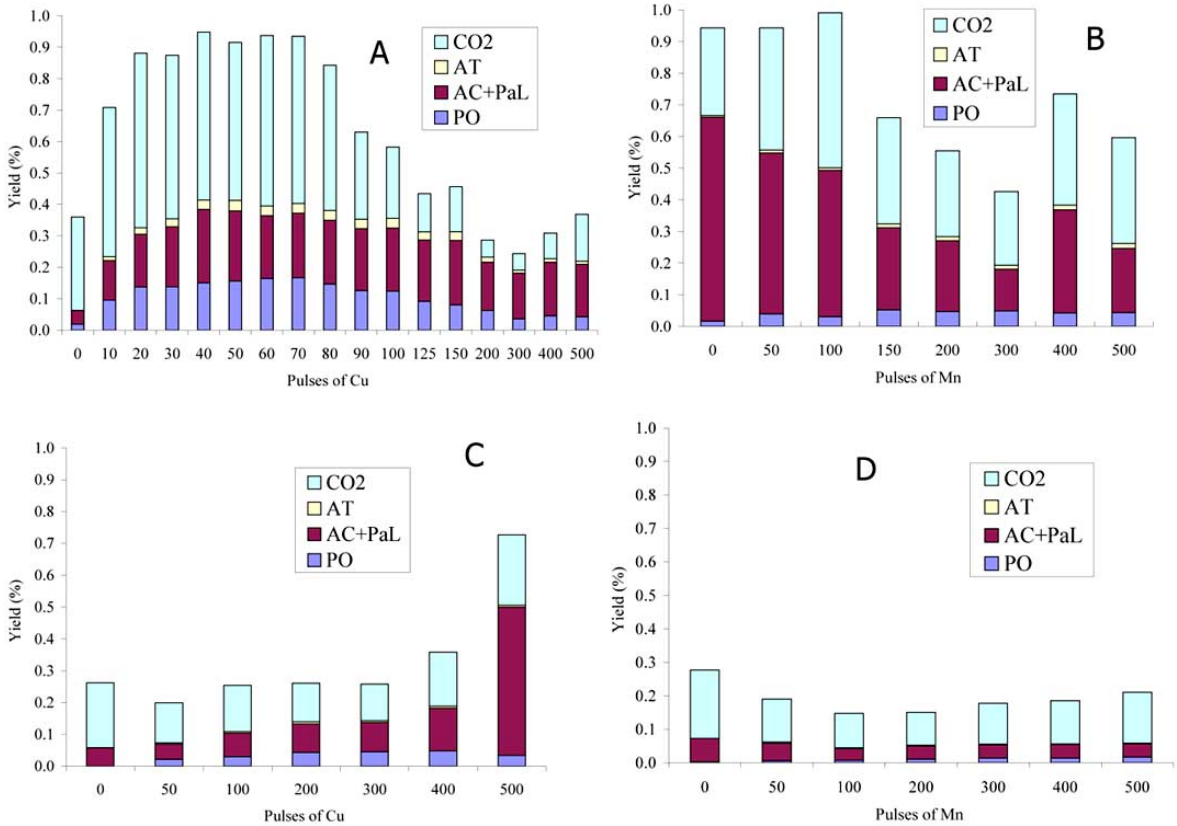

Fig. (6). Product yield results at 375°C for (**A**): bimetallic Cu-on-Mn/SiO_2, (**B**): bimetallic Mn-on-Cu/SiO_2, (**C**): unimetallic Cu/SiO_2, (**D**): unimetallic Mn/SiO_2. The yield of PO in (**A**) is increased about 5 fold over unimetallic catalyst variations. AT=acetone, AC=acrolein, PaL=propionaldehyde (trace amounts), PO=propylene oxide.

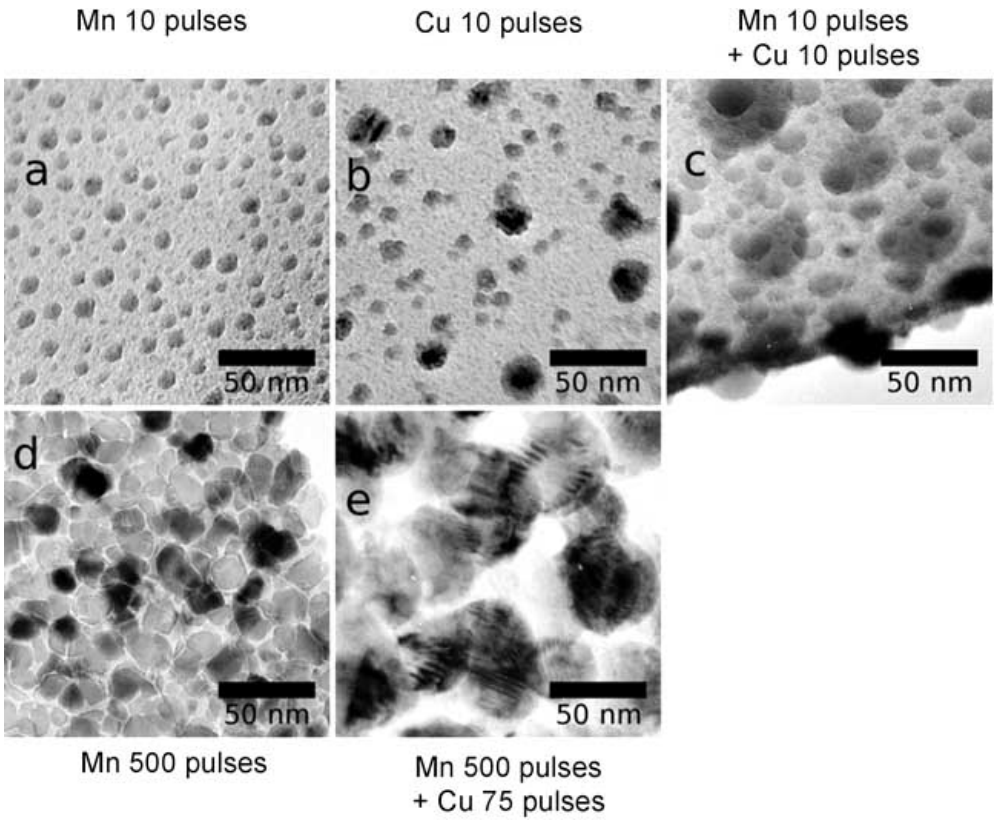

Fig. (7). TEM images of nanoparticles of 10 pulses of Mn (**A**), 10 pulses of Cu (**B**), 10 pulses of Mn followed by 10 pulses of Cu (**C**), 500 pulses of Mn (**D**), and 500 pulses of Mn followed by 75 pulses of Cu (**E**). The last image also corresponds to the catalyst that led to the production of highest levels of PO reported here.

In an effort to provide insights on the morphology of the Mn+Cu catalysts, TEM images of their nanoparticles were also determined, and are shown in Fig. (**7**). As seen from this figure, nanoparticle growth at higher pulse numbers was evident both for Mn and Cu. However, for the case of Cu, particle growth was more significant than Mn, as seen in Fig. (**7E**, **D**), respectively.

In summary, High Throughput PLA synthesis and reaction screening of supported metal nanoparticles resulted in the discovery of improved bimetallic Cu-on-Mn/SiO_2 catalyst leads for the direct synthesis of PO from propylene and oxygen. It has been demonstrated that multimetallic systems can exhibit synergistic catalytic effects, boosting the desired PO yields by several fold with the observed synergy depending on the sequence of deposition. This discovery calls for the undertaking of detailed follow-up studies to optimize both the catalyst preparation process and the reactor operating conditions (e.g., residence time, temperature, etc.) to fully explore the limits of the Mn+Cu bimetallic system in direct PO synthesis. These results also illustrate the importance of exploring multimetallic systems and the useful role High Throughput methods play in catalyst research and development.

ACKNOWLEDGEMENTS

We are grateful to the UCLA Materials Creation and Training Program (MCTP) for a fellowship to Michael Kahn. We also thank Laboratory Catalyst Systems LLC for funding and the use of their facilities.

REFERENCES

[1] Matar, S.; Hatch, L.F. *Chemistry of Petrochemical Processes*; Gulf Publishing Company: Houston, Texas, **1994**.

[2] Nijhuis, T.A.; Makkee, M.; Moulijn, J.A.; Weckhuysen, B.M. The production of propene oxide: Catalytic processes and recent developments. *Ind. Eng. Chem. Res.*, **2006**, *45*(10), 3447-3459.

[3] Bettahar, M.M.; Costentin, G.; Savary, L.; Lavalley, J.C. On the partial oxidation of propane and propylene on mixed metal oxide catalysts. *Appl. Catal. A Gen.*, **1996**, *145*(1-2), 1-48.

[4] Monnier, J.R. The direct epoxidation of higher olefins using molecular oxygen. *Appl. Catal. A Gen.*, **2001**, *221*(1-2), 73-91.

[5] Lu, G.Z.; Zuo, X.B. Epoxidation of propylene by air over modified silver catalyst. *Catal. Lett.*, **1999**, *58*(1), 67-70.

[6] Murata, K.; Liu, Y.Y.; Mimura, N.; Inaba, M. Epoxidation of propylene with molecular oxygen/methanol over a catalyst system containing palladium and Ti-modified MCM-22 without hydrogen. *J. Catal.*, **2003**, *220*(2), 513-518.

[7] Stangland, E.E.; Stavens, K.B.; Andres, R.P.; Delgass, W.N. Characterization of gold-titania catalysts via oxidation of propylene to propylene oxide. *J. Catal.*, **2000**, *191*(2), 332-347.

[8] Sinha, A.K.; Seelan, S.; Akita, T.; Tsubota, S.; Haruta, M. Vapor phase propylene epoxidation over Au/Ti-MCM-41 catalysts prepared by different Ti incorporation modes. *Appl. Catal. A Gen.*, **2003**, *240*(1-2), 243-252.

[9] Wang, R.P.; Guo, X.W.; Wang, X.S.; Hao, J.Q.; Li, G.; Xiu, J.H. Effects of preparation conditions and reaction conditions on the epoxidation of propylene with molecular oxygen over Ag/TS-1 in the presence of hydrogen. *Appl. Catal. A Gen.*, **2004**, *261*(1), 7-13.

[10] Yap, N.; Andres, R.P.; Delgass, W.N. Reactivity and stability of Au in and on TS-1 for epoxidation of propylene with H_2 and O_2. *J. Catal.*, **2004**, *226*(1), 156-170.

[11] Zwijnenburg, A.; Makkee, M.; Moulijn, J.A. Increasing the low propene epoxidation product yield of gold/titania-based catalysts. *Appl. Catal. A Gen.*, **2004**, *270*(1-2), 49-56.

[12] Dai, M.H.; Tang, D.L.; Lin, Z.J.; Yang, H.W.; Yuan, Y.Z. Ti-Si mixed oxides by non-hydrolytic sol-gel synthesis as potential gold

catalyst supports for gas-phase epoxidation of propylene in H_2 and O_2. *Chem. Lett.*, **2006**, *35*(8), 878-879.

[13] Chowdhury, B.; Bravo-Suárez, J.J.; Daté, M.; Tsubota, S.; Haruta, M. Trimethylamine as a gas-phase promoter: highly efficient epoxidation of propylene over supported gold catalysts. *Angew. Chem. Int. Ed.*, **2006**, *45*(3), 412-415.

[14] a) Vaughan, O.P.H.; Kyriakou, G.; Macleod, N.; Tikhov, M.; Lambert, R.M. Copper as a selective catalyst for the epoxidation of propene. *J. Catal.*, **2005**, *236*(2), 401-404. b) Torres, D.; Lopez, N.; Illas, F.; Lambert, R.M. Low-basicity oxygen atoms: a key in the search for propylene epoxidation catalysts. *Angew. Chem. Int. Ed.*, **2007**, *46*(12), 2055-2058.

[15] Song, Z.X.; Mimura, N.; Bravo-Suarez, J.J.; Akita, T.; Tsubota, S.; Oyama, S.T. Gas-phase epoxidation of propylene through radicals generated by silica-supported molybdenum oxide. *Appl. Catal. A Gen.*, **2007**, *316*(2), 142-151.

[16] Orzesek, H.; Schulz, R.P.; Dingerdissen, U.; Maier, W.F. Selective oxidation of propene with air to propylene oxide, a case study of autoxidation versus catalytic oxidation with AMM-catalysts. *Chem. Eng. Technol.*, **1999**, *22*(8), 691-700.

[17] Senkan, S. Combinatorial heterogeneous catalysis - a new path in an old field. *Angew. Chem. Int. Ed.*, **2001**, *40*(2), 312-329.

[18] Senkan, S.; Ozturk, S. Discovery and optimization of heterogeneous catalysts by using combinatorial chemistry. *Angew. Chem. Int. Ed.*, **1999**, *38*(6), 791-795.

[19] Senkan, S.; Krantz, K.; Ozturk, S.; Zengin, V.; Onal, I. High-throughput testing of heterogeneous catalyst libraries using array microreactors and mass spectrometry. *Angew. Chem. Int. Ed.*, **1999**, *38*(18), 2794-2799.

[20] Duan, S.; Kahn, M.; Senkan, S. High-throughput nanoparticle catalysis: Partial oxidation of propylene. *Comb. Chem. High Throughput Screen.*, **2007**, *10*(2), 111-119.

[21] Senkan, S.; Kahn, M.; Duan, S.; Ly, A.; Leidhom, C. High-throughput metal nanoparticle catalysis by pulsed laser ablation. *Catal. Today*, **2006**, *117*(1-3), 291-296.

[22] Mirodatos, C.; Maier, W.F.; Aresta, M. Recent developments in combinatorial catalysis research and high-throughput technologies - Preface. *Catal. Today*, **2008**, *137*(1), 1-1.

[23] Farrusseng, D. High-throughput heterogeneous catalysis. *Surf. Sci. Rep.*, **2008**, *63*(11), 487-513.

[24] Margitfalvi, J.L. Combinatorial heterogeneous catalysis. *Comb. Chem. High Throughput Screen*, **2007**, *10*(2), 83-84.

[25] Lamb, A.B.; Bray, W.C.; Frazer, J.C.W. The removal of carbon monoxide from air. *J. Ind.. Eng. Chem.*, **1920**, *12*(3), 213-221.

[26] Musick, J.K.; Williams, F.W. Catalytic decomposition of halogenated hydrocarbons over hopcalite catalyst. *Ind. Eng. Chem. Prod. Res. Dev.*, **1974**, *13*(3), 175-179.

Received: January 30, 2009 **Revised: April 13, 2009** **Accepted: May 4, 2009**